The Interaction of Supernova Blast Waves with Interstellar clouds: Experiments on the Omega Laser

Richard I. Klein
University of California LLNL and
Berkeley, Department of Astronomy

Collaborators
Harry Robey, Ted Perry, Jave Kane, Jeff Greenough,
Marty Marinak

Lawrence Livermore National Laboratory

Four Stages of Shock-Sphere Interaction

- Initial development of reflected, transmitted and diffracted shocks
- Shock compression, convergence and multiple shock interaction ⇒ triple point flow and vorticity production
- Re-expansion and shear flow instabilities
- Destruction by instabilities and differential forces

The interaction of shock waves with clouds in the ISM is a problem of fundamental importance

Composite image from the ROSAT satellite

Graham *et al.*, ApJ 1997

yellow = X ray
blue = H-α
green = H-α + OIII + X ray

Shock waves from supernovae

shocks heat the coronal phase of the ISM

determine the velocity dispersion of clouds

↓

governs the scale height of the ISM

may effectively destroy clouds

↓

mixing of clouds with ISM

compression of clouds

↓

gravitational collapse

↓

star formation

Kimberly S. Budil *et al.*, *1998 Joint APS/AAPT Meeting*

KLEIN et al. 1990, 1994, 1995, 1996, 1999, 2000, 2001
Zabusky (??)

There is ample evidence of the aftermath of shock-cloud interations in the Cygnus Loop supernova remnant

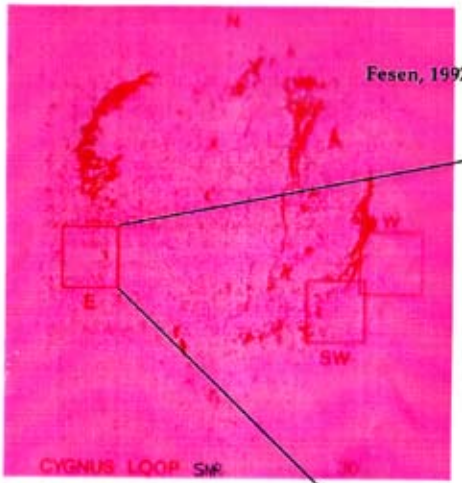

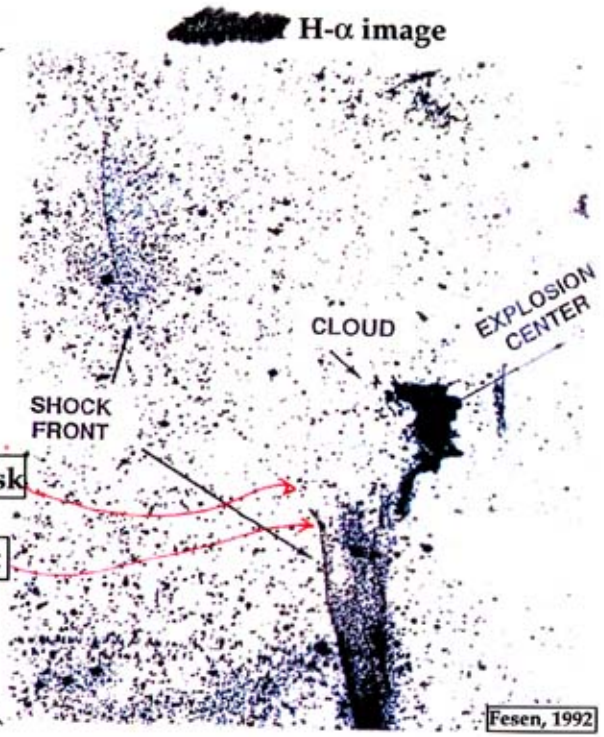

$R_{cloud} \sim 0.5$ pc

$n_{cloud} \sim 1$

$R_{shock} \sim 5.2 \times 10^{18}$

$v_{shock} \sim 4 \times 10^{7}$ cm/s

$t \sim 4.1 \times 10^{3}$ year

Understanding and Modeling the Evolution of 3D Hydrodynamic Instabilities and Turbulence is Crucial for Code Validation

- The shock-sphere experiments are rich in shock physics relevant to code validation
  - Multiple shock structure interactions from reflected, transmitted, diffracted shocks
  - Multiple shock-shock interactions with Mach stems, triple points, shear flows
  - Non-Linear hydrodynamics instabilities such as R-M, R-T, K-H
  - Vortex ring instabilities (bending mode) that cause large-scale vorticity and mixing
  - Turbulent flows

Timescales continued

Pressures comparable

$$V_s \approx (\rho_{Io}/\rho_{co})^{1/2} V_b \text{(non radiative)}$$

if $\dot{V}_s, \dot{V}_b < 0 \Rightarrow$ accurate to ≈ 1.5

if shock is radiative $\rho_{I1} >> \rho_{I0}$ typically $\rho_{I1} \gtrsim \rho_{I0}$

$\Rightarrow V_s$ (radiative) $>> V_s$ (non-radiative)

Timescale for shock to sweep across sphere

$$t_{ic} \equiv \frac{2a_o}{V_b}$$ Intercloud Crossing time

Timescale for sphere to be crushed by shock moving into the sphere

$$t_c \equiv \frac{a_o}{V_s} = \frac{\chi^{1/2} a_o}{V_b}$$ Cloud Crushing Time

t_c is the basic timescale governing the evolution of the sphere

$\{\chi, m\}$ characterize evolution $\Rightarrow$ scaling

After the shock has swept over the sphere, the shocked sphere is subject to Kelvin-Hemholtz and Rayleigh-Taylor instabilities

For $\chi >> 1$, the time-scale t_{KH} for growth of K-H instabilities for perturbations of wavenumber k parallel to relative V_{rel} between sphere and surrounding medium is

$$t^{-1}_{KH} = k\, v_{rel}/\chi^{1/2}$$

$$\Rightarrow \frac{t_{KH}}{t_c} = \frac{V_b / V_{rel}}{ka_o} \rightarrow \text{K-H growth time-tc,}$$

Shortest wavelength cause the fastest growth

It can also be shown for Rayleigh-Taylor

$$\Rightarrow \frac{t_{RT}}{t_c} \cong \frac{1}{(ka_o)^{1/2}} \Rightarrow \text{sphere undergoes severe instabilities in few } t_c$$

SNR age

For Sedov-Taylor

Blast Wave $t \equiv \frac{\alpha R_b}{V_b} = \frac{2}{5}\frac{R_b}{V_b}$ $\left(V_b = \frac{dR_b}{dt} = \alpha t^{\alpha-1}\right)$

$R_{blast} \propto t^{\alpha}\ (\alpha = 2/5)$

If $\chi >> 1 \Rightarrow t_{cc} > t_{ic}$, Clouds are characterized in 3 sizes

Small clouds $t > t_{cc} \Rightarrow a << \frac{0.1R}{\chi^{1/2}}$

SNR does not evolve significantly during cloud crushing – cloud is promptly crushed. V_s ~ constant pressure on cloud ≈ steady.

Medium clouds $t_{cc} > t > t_{lc} \Rightarrow \frac{0.1R}{\chi^{1/2}} < a < 0.05R$ V_s decelarated

Blast wave does evolve during the time to crush the cloud.

Large clouds $t < t_{lc} \Rightarrow a > 0.05R$

Blast wave weakens significantly over time to cross clouds

Force on clouds impulsive

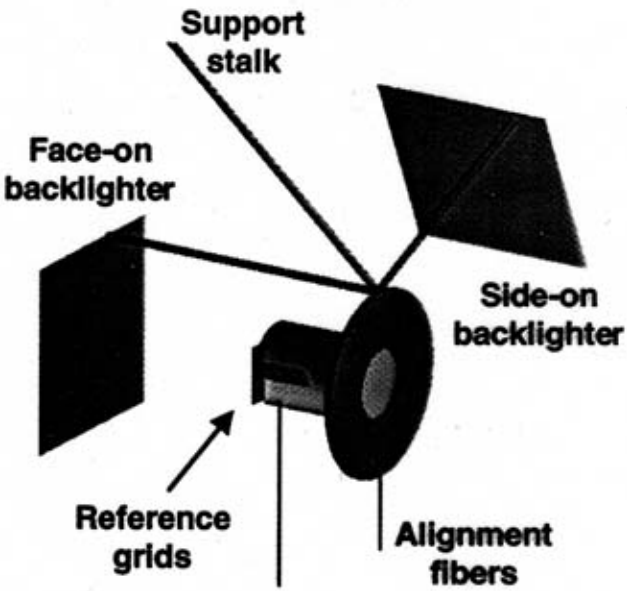

Figure 1(b), Robey, Phys. Rev. Lett.

Experimental Setup

- Achieve strong shock conditions with direct 10 beams with 500 J/beam, flat pulse length 10 ns and laser wavelength of 0.351 μm onto target
- Beams have super-Gaussian spatial intensity

$$I/Io = \exp\ [-(r/412\ \mu m)]^{4.7}$$

- Target Diameter is 800 μm
- Berryllium shield was used to delay shock propagation around target and generate planar shock propagation.
- Direct -drive laser illumination used to permit face-on imagining of target

⇒ Previous experiments (Klein et al. 2000 - 2001) used indirect-drive

Experimental Setup - con't

- Cu sphere with 120 μm diameter (**representing interstellar cloud**) and density 8.95g/cm^3 embedded in Beryllium shock tube filled with polystyrene (CH) at density 1.044g/μm^3 (**representing interstellar medium**)
- Interaction is imaged with 5.2 KeV x-rays with 7 additional Omega beams

Experimental Setup - con't

- Advantages of indirect-Drive $\Rightarrow$ produces a more uniform radiation flux and shocks of greater planarity
- Disadvantages: Plasma blown off the walls prohibits late-time imaging of interaction from face-on direction.
- Direct-Drive maintains face-on access for duration of the experiment

Experimental Radiographs

Side-on Face-on

t = 13 ns
shock passes
over sphere

t = 26 ns
shock is
well passed
sphere

t = 39 ns
shock is out
of field of view

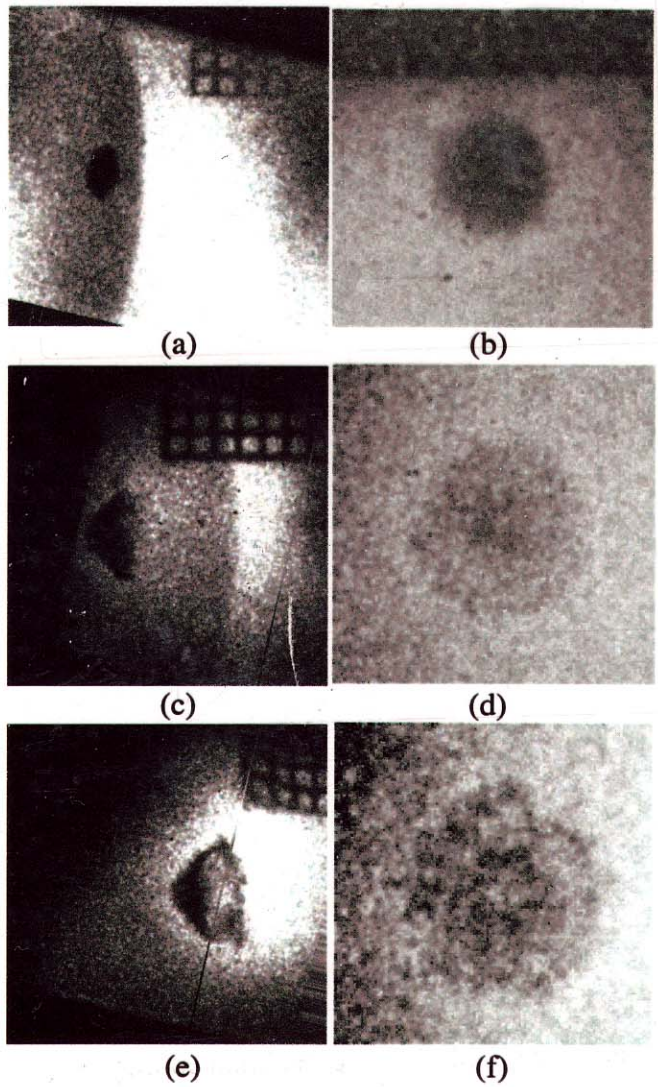

Figure 2, Robey, Phys. Rev. Lett.

Experimental Results

- Experimental radiographs show interaction with "simultaneous" side-on and face-on images

t=12 ns

- Sphere compressed in axial direction with little radial compression

t=26 ns

- Sphere undergoes severe axial compression. Baroclinic vorticity generated at sphere-CH interface

- Vorticity generated during initial passage of shock over spherical cloud

Experimental Results - con't

- Vorticity generated during subsequent post-shock flow at cloud-intercloud boundary
- Flow around cloud produces high-pressure Mach reflected shock into back side of cloud
- Side shocks weaker than front and aft shocks due to pressure minimum at sides

$\Rightarrow$ Results in strong axial compression - sphere begins to pancake

Experimental Results - con't

- Emergence of double ring structure seen in face-on radiograph

t=39ns

- Strong vortex roll up noted on sides of sphere
- Face-on view shows distinct double ring structure which tracks development of double vortex ring
  - Klein and McKee (1994) showed that 3-D vorticity field of cloud is well tracked by full density field ⇒ Vortex Ring Instability

Azimuthal line-outs from face-on images of shock / sphere interaction at t = 39 ns

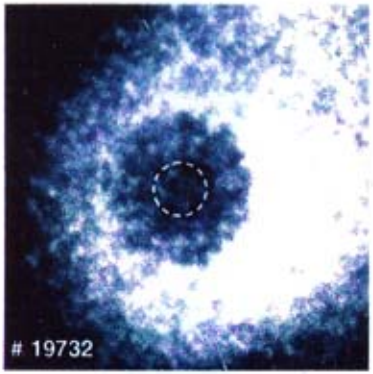

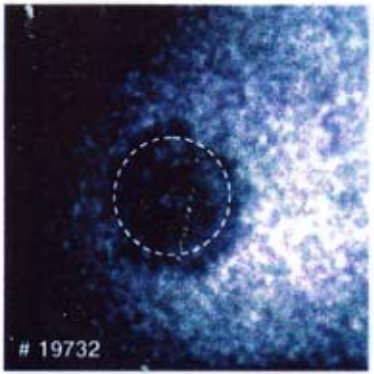

Azimuthal line-out
through central feature (r=36 μm)

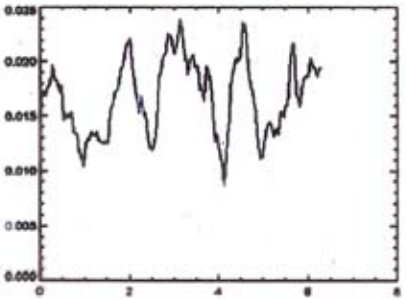

Azimuthal line-out
through outer feature (r=80 μm)

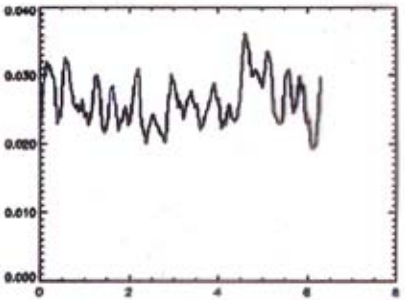

Modal Analysis of Double Vortex Ring at t = 39 ns

Double Vortex Ring structure

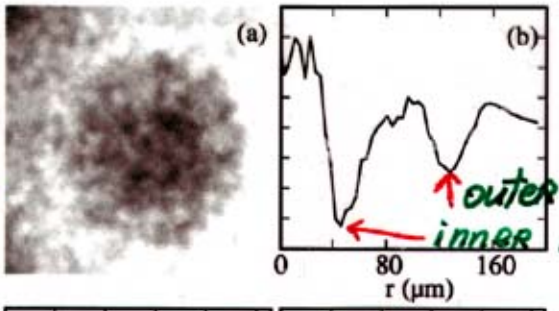

radial transparency of double ring

Azimuthal mode structure
Azimuthal Lineouts

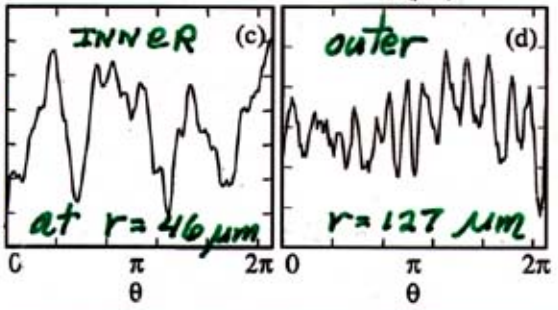

Power Density spectrum of Azimuthal Lineouts

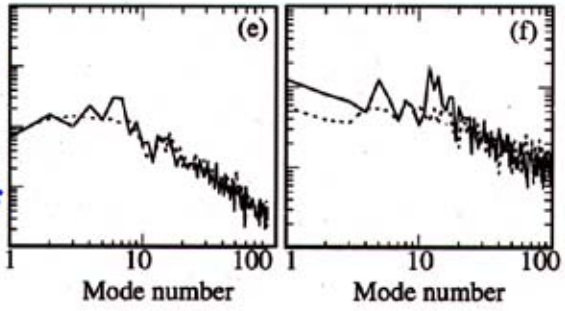

INNER Vortex Ring Dominant mode n = 5-8

OUTER Vortex Ring Dominant mode n = 15

Figure 3, Robey, Phys. Rev. Lett.

Modal Analysis of Double Vortex Ring Structure

- 3-D simulations show development of 2 Vortex Rings associated with cloud that undergo bending mode instability (Klein and McKee, 1994; Marinak, Klein and Perry 2001)
- Azimuthally averaged radial lineouts of experimental radiograph show unambiguous double ring structure
- Azimuth lineouts at radial location of each ring show periodic azimuthal modulation suggesting a dominant mode number of 5 for inner ring and higher mode number of 14-16 for the outer ring

Modal Analysis of Double Vortex Ring Structure - con't

- Power density spectrum of azimuthal lineouts confirm dominant mode number of 5-8 for inner ring and dominant mode number 15 for outer ring

Experimental-Theoretical Comparison of Vortex Ring Modal Structure

- At t=39ns, shocks have left sphere and sphere advects essentially as an incompressible fluid
- Applying incompressible theory to describe an incompressible bending mode instability in vortex ring to experimental face-on radiographs $\Rightarrow$ dominant unstable mode for inner ring n=5-7 and n=15-17 for outer ring
- Theoretically determined dominant modes in non-axisymmetric unstable vortex rings are in remarkable agreement with experimentally determined unstable modes

Contours showing location of Inner and Outer Vortex Rings

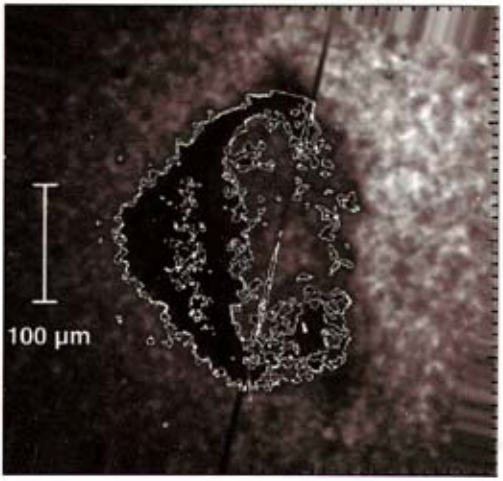

Figure 4, Robey, Phys. Rev. Lett.

3-D High Resolution AMR Simulations

- Side on view of simulation shows well separated front and back part of the sphere due to instabilities
- Side on view models inner transparent bubble seen in experimental radiograph
- Face on view shows clear evidence of inner and outer vortex rings seen in experimental radiograph
- Inner ring shows low mode structure and outer ring shows high mode structure as in radiographs
- Overall morphology of 3-D simulations in excellent agreement with experimental radiographs

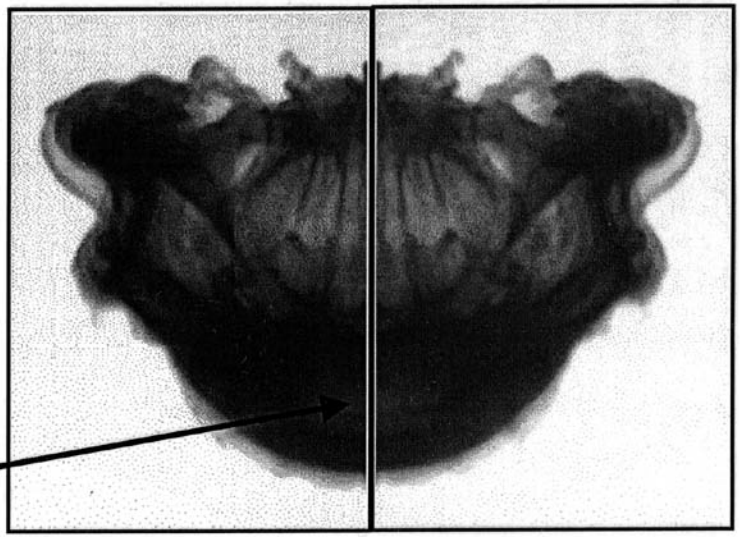

Figure X(a)

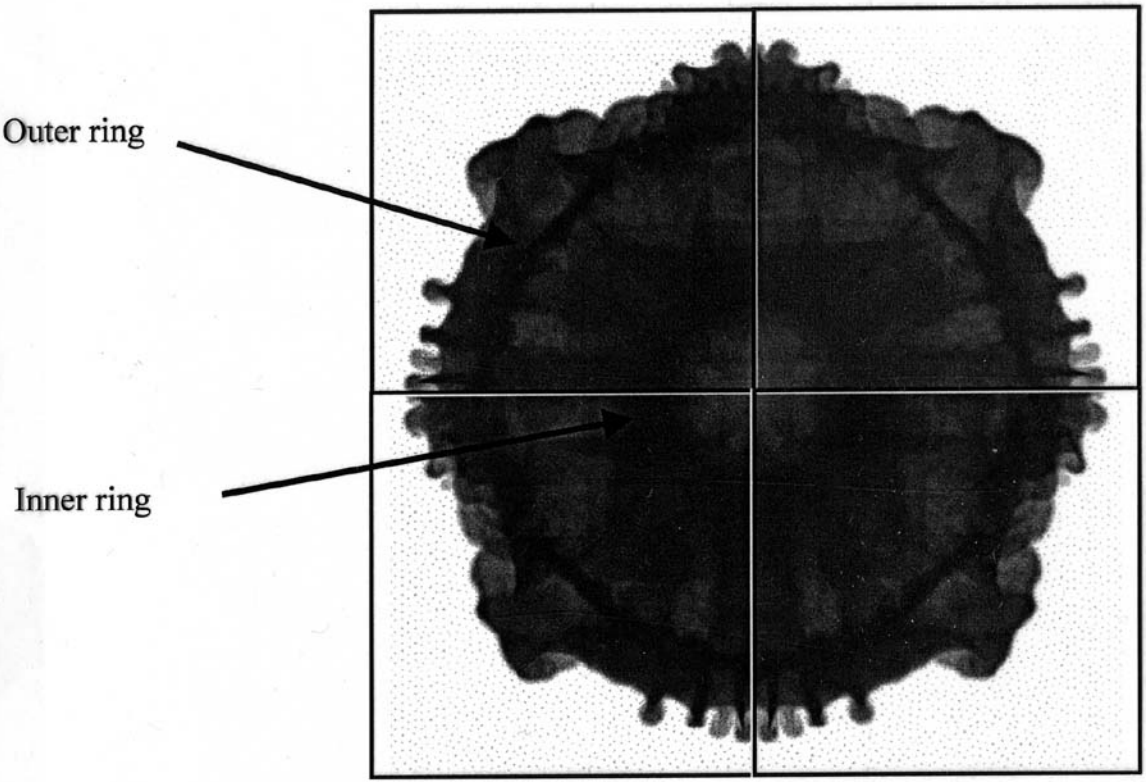

Figure X(b)

Conclusions

- The interaction of a supernova blast wave with interstellar clouds can be well scaled to an HED Omega laser experiment
- Development of vortex flow gives rise to strong vortex rings unstable to Widnall Bending Mode instabilities. **These are shown for the first time in HED laser experiment**
- At 39 ns (~3 t_c) hydrodynamic instabilities (R-T, K-H and Widnall) destroy sphere (cloud) resulting in turbulent mixing of cloud with surrounding medium (ISM)
- Power density spectrum of face-on radiographs determine dominant mode of inner and outer vortex rings to be n = 5-8 and n = 15
- Incompressible vortex ring theory shows remarkable agreement in predicting dominant unstable modes of vortex rings
- High resolution 3-D AMR simulations capture all essential morphological features of side-on and face-on experimental radiographs including appearance of double vortex rings